The Effect of Own Weight on Dynamic Analysis of a Pre-Stretched Composite Plate-Strip Containing Twin Circular Inclusions Under Bending Using Finite Element Method

*Ulku Babuscu Yesil

Yildiz Technical University, Faculty of Chemical and Metallurgical Engineering, Department of Mathematical Engineering, 34210, Istanbul, Turkey, ubabuscu@yildiz.edu.tr, (iD)

Abstract

This manuscript describes how the weight of a simply supported composite plate-strip (containing twin circular inclusions) affects its dynamic behaviors when exposed to bending load as analyzed via the finite element method (FEM). The centers of the twin circular inclusions are on a line parallel to the free surface, and the materials of both inclusions are the same. First, the effects of body forces (the plate-strip's own weight) and surface forces (pre-stretching load) on the plate-strip (both are considered to be initial stresses) are identified using the classical linear theory of elasticity. Next, the consequences of these stressors (identified in the first step) under additional time harmonic bending load on the forced vibration around the inclusions are determined using the three-dimensional linearized theory of elasticity (TDLTE) under the plane-strain state. The data herein suggest that the plate-strip's weight can significantly effect dynamic characteristics of the considered plate-strip.

Keywords: initial stress, own weight, circular inclusions, forced vibration, fundamental frequency

1. INTRODUCTION

The presence of inhomogeneities or defects (e.g., inclusions and holes) in structures affects their mechanical and physical properties, resulting in unwanted strain or stress. It is very important, however, that these strains and stresses remain within defined limits for the structure's security. Several studies have been conducted on the stresses and strains caused by inclusions (Mura [1], Mura et al. [2] and Zhou et al. [3]). Hufenbach and Zhou [4] developed a solution method for the anisotropic elastic host; this was obtained via engineering mechanics with the boundary collocation technique. In this solution method, all of the stresses and displacements were calculated under the assumption that corresponding displacements and stresses of the constituents of the plate are equal on the contact surfaces, linear elasticity, and a plane strain state. Huang [5] utilized the Mori-Tanaka mean-field method to determine the effect of fiber aspect ratio on the effective elastic modulus of composites.

Detailed studies have reported the effect of initial stretching on a plate with twin inclusions on forced vibration analysis in Babuscu Yesil [6] and Akbarov [7]. However, these previous studies did not take into account the object's weight, and therefore, all structures (both heavy and light) were considered equal. However, in order to have a safe structure, the structure's weight must be taken into account. Some studies have identified the structure's weight as the 'dead

load.' Dead loads are modelled as loads that are unchanging, and are thought to play a key role in structural collapse [8-11]. Therefore, researchers must take into account the influence of dead loads in order to obtain better results and more stable structures. Previous studies [8-11] that performed dynamic analyses on plates and beams with an approximate closed-form solution of the structures took the influence of dead loads into account. The effect of the weight of a pre-stretched plate-strip containing a circle-shaped hole on static analysis were studied in Babuscu Yesil [12]. Other studies analyzed the effect of dead load on the dynamic behaviors of beams Zhou and Zhu [13] and plates Zhou [14] using the concept of load-induced stiffness matrix via the finite-element method.

The current study describes the effect of its own weight on a plate-strip containing twin circle shaped inclusions on dynamic analyses under uniformly distributed time harmonic bending forces. The plate-strip includes twin circular inclusions whose centers are on a line parallel to the free surface and made from the same materials. The harmonic bending forces were applied to the top of the pre-stretched plate-strip. The problem is modelled via TDLTE in the plane-strain state, and the problem is numerically solved via the FEM. Based on a literature search, this is the first attempt to introduce the effect of own weight of a structure containing inclusions on dynamic analysis.

*[1]Corresponding Author: Yildiz Technical University, Faculty of Chemical and Metallurgical Engineering, Department of Mathematical Engineering, Istanbul, Turkey, ubabuscu@yildiz.edu.tr, (+90) 212 383 4606

2. PROBLEM FORMULATION AND COMPUTATIONAL TECHNIQUE

Considering that the plate-strip's own weight (intensity f) and uniaxial stretching forces (intensity q) act together, there were two forces being applied to the plate-strip in the reference (initial) state. The effect between the stretching force and the body force on the distribution of stresses, strains, and displacements of the plate-strip were determined with the classical linear theory of elasticity using the superposition principle.

The effect of the simply supported plate-strip's own weight on the dynamic characteristics at its ends (i.e., $x_1 = 0$ and $x_1 = L$) was analyzed by the finite element method. Uniformly distributed normal stretching forces of intensity q act on the plate-strip's ends, and body forces of intensity f act on the plate-strip in its initial state. Moreover, there is no force applied on the plate-strip inside the inclusions, and additional uniformly distributed dynamic (time harmonic) normal forces of amplitude p ($\ll$ q and ($\ll$ f) work on the top of the plate-strip (Fig. 1). The radius of the inclusions is denoted as 'R,' the width of the plate-strip as 'L,' and the height of the plate-strip as 'H'.

The problem can be solved in two parts as follows: 1) the initial (reference) part, and 2) the perturbed part. In the initial part, the plate-strip's displacement and stress distributions are analyzed using the effect between the uniformly distributed uniaxial stretching force and body force. These are initial values, and the quantities of the reference part will be denoted by the superscript (0). During the second (perturbed) part, the results of the first part will be considered, and then displacement and stress distributions will be determined for the pre-stressed plate-strip using uniformly distributed dynamic bending forces.

Fig. 1 reveals a sketch of the plate-strip containing twin circular inclusions and associate with this plate-strip the Cartesian coordinate system Ox_1x_2; the Ox_3 axis is directed normally along the Ox_1x_2 plane.
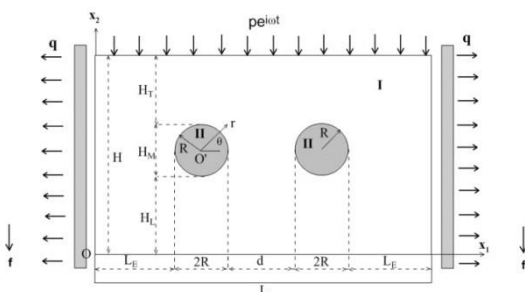

Fig. 1. Plate-strip containing twin circular inclusions.
The mathematical formulations of the considered boundary value problems for both parts are given below:

For initial (Reference) Part:

$$\frac{\partial \sigma_{ij}^{(0),k}}{\partial x_j} + f_i = 0, f_i = \rho g \delta_2^i \tag{1}$$

$$\sigma_{11}^{(0),k} = (\lambda_k + 2\mu_k)\varepsilon_{11}^{(0),k} + \lambda_k \varepsilon_{22}^{(0),k}$$
$$\sigma_{22}^{(0),k} = \lambda_k \varepsilon_{11}^{(0),k} + (\lambda_k + 2\mu_k)\varepsilon_{22}^{(0),k} \tag{2}$$
$$\sigma_{12}^{(0),k} = 2\mu_k \varepsilon_{12}^{(0),k}$$

$$\varepsilon_{ij}^{(0),k} = \frac{1}{2}\left(\frac{\partial u_i^{(0),k}}{\partial x_j} + \frac{\partial u_j^{(0),k}}{\partial x_i}\right) \tag{3}$$

$$u_2^{(0),1}\Big|_{\substack{x_1=0;L \\ x_2\in[0,H]}} = 0$$
$$\sigma_{11}^{(0),1}\Big|_{\substack{x_1=0;L \\ x_2\in[0,H]}} = q\delta_1^i$$
$$\sigma_{12}^{(0),1}\Big|_{\substack{x_1=0;L \\ x_2\in[0,H]}} = 0 \tag{4}$$
$$\sigma_{i2}^{(0),1}\Big|_{\substack{x_2=0;H \\ x_1\in[0,L]}} = 0$$

$$u_i^{(0),1}\Big|_{I_L} = u_i^{(0),2}\Big|_{I_L}$$
$$u_i^{(0),1}\Big|_{I_R} = u_i^{(0),2}\Big|_{I_R}$$
$$\sigma_{ji}^{(0),1} n_j\Big|_{I_L} = \sigma_{ji}^{(0),2} n_j\Big|_{I_L} = 0 \tag{5}$$
$$\sigma_{ji}^{(0),1} n_j\Big|_{I_R} = \sigma_{ji}^{(0),2} n_j\Big|_{I_R} = 0$$

For Perturbed Part:

$$\frac{\partial}{\partial x_j}\left(\sigma_{ji}^k + \sigma_{in}^{(0),k}\frac{\partial u_i^k}{\partial x_n}\right) = \rho \frac{\partial^2 u_i^k}{\partial t^2} \tag{6}$$

$$\sigma_{11}^k = (\lambda_k + 2\mu_k)\varepsilon_{11}^k + \lambda_k \varepsilon_{22}^k,$$
$$\sigma_{22}^k = \lambda_k \varepsilon_{11}^k + (\lambda_k + 2\mu_k)\varepsilon_{22}^k, \tag{7}$$
$$\sigma_{12}^k = 2\mu_k \varepsilon_{12}^k$$

$$\varepsilon_{ij}^k = \frac{1}{2}\left(\frac{\partial u_i^k}{\partial x_j} + \frac{\partial u_j^k}{\partial x_i}\right) \tag{8}$$

$$u_2^1\Big|_{\substack{x_1=0;L \\ x_2\in[0,H]}} = 0$$
$$\left(\sigma_{j1}^1 + \sigma_{1n}^{(0),1}\frac{\partial u_1^1}{\partial x_n}\right)n_j\Bigg|_{\substack{x_1=0;L \\ x_2\in[0,H]}} = 0$$
$$\left(\sigma_{ji}^1 + \sigma_{in}^{(0),1}\frac{\partial u_i^1}{\partial x_n}\right)n_j\Bigg|_{\substack{x_2=H \\ x_1\in[0,L]}} = pe^{i\omega t}\delta_2^i \tag{9}$$
$$\left(\sigma_{ji}^1 + \sigma_{in}^{(0),1}\frac{\partial u_i^1}{\partial x_n}\right)n_j\Bigg|_{\substack{x_2=0 \\ x_1\in[0,L]}} = 0$$

$$u_i^1\Big|_{I_L} = u_i^2\Big|_{I_L}$$
$$u_i^1\Big|_{I_R} = u_i^2\Big|_{I_R}$$
$$\left(\sigma_{ji}^1 + \sigma_{in}^{(0),1}\frac{\partial u_i^1}{\partial x_n}\right)n_j\Bigg|_{I_L} = \left(\sigma_{ji}^2 + \sigma_{in}^{(0),2}\frac{\partial u_i^2}{\partial x_n}\right)n_j\Bigg|_{I_L} = 0 \tag{10}$$
$$\left(\sigma_{ji}^1 + \sigma_{in}^{(0),1}\frac{\partial u_i^1}{\partial x_n}\right)n_j\Bigg|_{I_R} = \left(\sigma_{ji}^2 + \sigma_{in}^{(0),2}\frac{\partial u_i^2}{\partial x_n}\right)n_j\Bigg|_{I_R} = 0$$

All of the recurring indices (i,j,k=1,2) are added up throughout their ranges utilizing the following code: σ_{ij}- stress, ε_{ij}- strain and u_i- displacement tensors. k=1 (k=2)

denotes the related values of the matrix's (inclusions') materials, f_i- refers to the constituent of the density of the body force, ρ refers to the mass density of the material in the plate-strip, g refers to the gravitational acceleration and δ_i^j- refers to the Kronecker symbol. $I_L(I_R)$- denotes the contour of the left (right) inclusion determined by Eq. (11), the Lame constants are denoted by λ_k and μ_k, t indicates time, and n_j refers to the constituents of the unit normal vector that is applied to the outline of the inclusions.

$$I_L = \left\{ x_1, x_2 | (x_1 - (L_E + R))^2 + (x_2 - (H_L + R))^2 = R^2 \right\}$$
$$I_R = \left\{ x_1, x_2 | \left(x_1 - (L - (L_E + R))\right)^2 + (x_2 - (H_L + R))^2 = R^2 \right\} \quad (11)$$

In the forced vibration problem, inhomogeneous part of the boundary condition at $x_2 = H$ is $pe^{i\omega t}$ and here p is constant. The perturbed part solution is formulated by Eqs. (6)-(10), and the solutions are determined by the following:

$$\{\sigma_{ij}, \epsilon_{ij}, u_i\} = \{\overline{\sigma}_{ij}, \overline{\epsilon}_{ij}, \overline{u}_i\} \exp(i\omega t) \quad (12)$$

where $\overline{\sigma}_{ij}, \overline{\epsilon}_{ij}$ and $\overline{u}_i$ indicate amplitudes. Eq. (12) can be applied to the motion Eq. (6), and after some manipulations, the equation below was developed in order to relate amplitudes:

$$\frac{\partial}{\partial x_j} \left(\overline{\sigma}_{ji}^{,k} + \sigma_{in}^{(0),k} \frac{\partial u_i^{,k}}{\partial x_n} \right) + \rho \omega^2 \overline{u}_i^{,k} = 0 \quad (13)$$

Eqs. (7)-(8) as well as the boundary and contact conditions (with the exception of $x_2 = H$) are similarly fulfilled for the matching amplitudes. However, the $x_2 = H$ conditions need to be replaced as shown below:

$$\left. \left(\overline{\sigma}_{ji}^{,1} + \sigma_{in}^{(0),1} \frac{\partial \overline{u}_i^{,1}}{\partial x_n} \right) n_j \right|_{\substack{x_2 = H \\ x_1 \in [0,L]}} = p\delta_2^i \quad (14)$$

Lastly, the perturbed part of the boundary value problem is represented with the Eqs. (13), (7-10), and (14).

3. PROCESS OF ARRIVING AT A SOLUTION

The numerical solution to the above problems will be determined using the FEM method. For this purpose, according to Akbarov (2013), Guz (1999) and (2004), the following functional will be used;

For the initial part of the boundary value problem:

$$\Pi^{(0)} = \frac{1}{2} \iint_{V'} \sigma_{ij}^{(0),1} \epsilon_{ij}^{(0),1} dx_1 dx_2 +$$
$$\frac{1}{2} \iint_{V_L} \sigma_{ij}^{(0),2} \epsilon_{ij}^{(0),2} dx_1 dx_2 + \frac{1}{2} \iint_{V_R} \sigma_{ij}^{(0),2} \epsilon_{ij}^{(0),2} dx_1 dx_2 - \quad (15)$$
$$\iint_V u_2^T f dx_1 dx_2 - \int_0^H q \, u_1^{(0),1} \Big|_{x_1=0} dx_2 + \int_0^H q \, u_1^{(0),1} \Big|_{x_1=L} dx_2$$

and for the perturbed part of the boundary value problem:

$$\Pi = \frac{1}{2} \iint_{V'} \left(T_{ij}^{,1} \frac{\partial \overline{u}_j^{,1}}{\partial x_i} + \rho \omega^2 \overline{u}_i^{,1} \overline{u}_j^{,1} \right) dx_1 dx_2 +$$
$$\frac{1}{2} \iint_{V_L} \left(T_{ij}^{,2} \frac{\partial \overline{u}_j^{,2}}{\partial x_i} + \rho \omega^2 \overline{u}_i^{,2} \overline{u}_j^{,2} \right) dx_1 dx_2 +$$
$$\frac{1}{2} \iint_{V_R} \left(T_{ij}^{,2} \frac{\partial \overline{u}_j^{,2}}{\partial x_i} + \rho \omega^2 \overline{u}_i^{,2} \overline{u}_j^{,2} \right) dx_1 dx_2 - \quad (16)$$
$$\int_0^L p \, \overline{u}_2^{,1} \Big|_{x_2=H} dx_1$$

where

$$T_{ij}^{,k} = \overline{\sigma}_{ij}^{,k} + \sigma_{in}^{(0),k} \frac{\partial \overline{u}_i^{,k}}{\partial x_n}, \qquad n; k; i; j = 1,2 \quad (17)$$

and V', V_L and V_R show the domains of solutions specified by Eqs.18

$$V' = V/(V_L \cup V_R)$$
$$V = V' \cup V_L \cup V_R = \{0 \le x_1 \le L, 0 \le x_2 \le H, -\infty \le x_3 \le \infty\}$$
$$V_L = \left\{ x_1, x_2 | (x_1 - (L_E + R))^2 + (x_2 - (H_L + R))^2 \le R^2 \right\}$$
$$V_R = \left\{ x_1, x_2 | \left(x_1 - (L - (L_E + R))\right)^2 + (x_2 - (H_L + R))^2 \le R^2 \right\} \quad (18)$$

In Eq. (17), $\sigma_{ij}^{(0)}$ is defined as the constituents of the initial stresses that were calculated from the boundary value problem of the initial part. Modeling via FEM for the initial part (perturbed part) of the boundary value problem is performed using the following equation:

Plate-strip's geometry and boundary conditions with respect to the planes $x_1 = L/2$, only the subdomain $V = \{0 \le x_1 \le L/2, 0 \le x_2 \le H\}$ which has been divided into a finite number of elements is taken into consideration, i.e., domain V is presented as $V = \cup_{n=1}^M V_n$ and V_n represents the area of the nth finite element and selected as curved triangular finite elements with 6 nodes (including the surrounding area of the inclusions and the inclusions domains) and biquadratic quadrilateral Lagrangian elements with 9 nodes (for the domain not included with the triangular elements) (Figs. 2a and 2b) [6], [18].
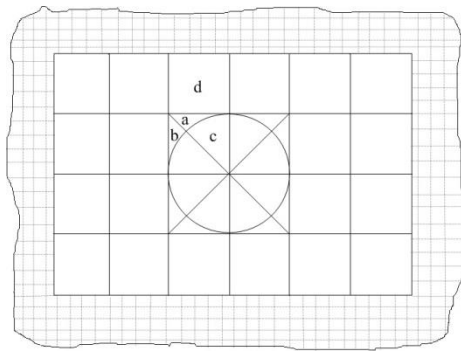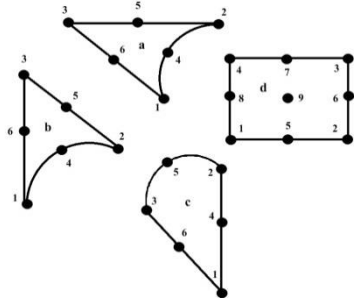
Fig. 2. (a) Finite Element Mesh

Fig. 2. (b) The configuration of various rectangular and triangular defined nodal elements.

The displacement-based formulation is used for the FEM modeling. The displacements in the defined elements' selected nodes are determined by employing the standard Ritz technique, which has been detailed in many references [17]. n^{th} FE displacement functions were chosen as follows:

For the initial part:

$$\mathbf{u}^{(0),k,n} \approx \mathbf{N}^{k,n}\mathbf{a}^{(0),k,n} \qquad (19)$$

For the perturbed part:

$$\mathbf{u}^{,k,n} \approx \mathbf{N}^{k,n}\mathbf{a}^{,k,n} \qquad (20)$$

In Eqs. (19) and (20),

$$\left(\mathbf{a}^{(0),k,n}\right)^{T} = \left\{u_{11}^{(0),k,n}, u_{21}^{(0),k,n}, \ldots, u_{1s}^{(0),k,n}, u_{2s}^{(0),k,n}\right\} \qquad (21)$$

$$\left(\mathbf{a}^{,k,n}\right)^{T} = \left\{u_{11}^{,k,n}, u_{21}^{,k,n}, \ldots, u_{1s}^{,k,n}, u_{2s}^{,k,n}\right\} \qquad (22)$$

$$\mathbf{N}^{k,n} = \left\{\begin{matrix} N_1^{k,n} & 0 & \ldots N_s^{k,n} & 0 \\ 0 & N_1^{k,n} & \ldots 0 & N_s^{k,n} \end{matrix}\right\} \quad \begin{matrix} n = 1,2,\ldots,M, \\ k = 1,2 \end{matrix} \qquad (23)$$

In Eqs. (21)-(23), the subscript s is taken 6 (9) for a triangular (rectangular) finite element; the superscript 'n' indicates defined elements V_n; while $\mathbf{N}^{k,n}$ are the shape functions defined at the nodes as biquadratic polynomial Lagrange shape functions for a quadrilateral defined element and second order polynomials for a triangular finite element whose unknown coefficients were determined using the following equation [17]:

$$N_i(x_{1j}, x_{2j}) = \delta_{ij} \qquad (24)$$

Substituting Eqs. (19) and (20) in the functionals (15) and (16) respectively, gives an algebraic equation system as given below:

For initial part,

$$\mathbf{K}^{(0)}\mathbf{a}^{(0)} = \mathbf{r}^{(0)} \qquad (25)$$

For perturbed part,

$$([\mathbf{K}] - \omega^2[\mathbf{M}])\mathbf{a} = \mathbf{r} \qquad (26)$$

$\mathbf{K}$ and $\mathbf{K}^{(0)}$ indicate the matrices of stiffness, $\mathbf{M}$ indicates the mass matrix, $\mathbf{a}$ and $\mathbf{a}^{(0)}$ indicate unknown nodal displacements, and $\mathbf{r}$ and $\mathbf{r}^{(0)}$ indicate the force vectors. The algebraic equations given in Eqs. (25) and (26) are solved to determine the displacement values at each node. Solving the equation for the perturbed part requires the distribution values of the stresses from the initial part, because Eq. (26) includes the initial part's stress values. They are obtained by solving Eq. (25) and then by using Hooke's Law.

Eq. (25) allows the determination of the displacement values at the nodes of the plate that subjected a static initial forces. Eq. (26) allows for the determination of the amplitudes of the displacement values at the nodes of the plate that was subjected to forced vibration; these values result from time-harmonic forces that act on the top of the plate-strip. On the other hand, the fundamental frequencies can be calculated from the following equation:

$$\det|\mathbf{K} - \omega^2\mathbf{M}| = 0 \qquad (27)$$

For this study, it is important to note that the study's author composed all of the computer programs used for the numerical calculations (using package FTN77). For both of the boundary value problems, the arrangements and meshing of finite elements are similar. To calculate the values for the definite integrals, the Gauss Quadrature method was employed, and included 10 sample points. For ease, and so that the numerical values around the circular inclusions could be better understood, the cylindrical coordinate system $(Or\theta x_3)$ was used to determine the stress values [12]).

4. NUMERICAL RESULTS

All of the numerical calculations in this study consider the fact that the plate-strip is composed of two isotropic materials (i.e., those making up the inclusions and the

matrix). The ideal contact conditions on the boundaries of these materials were satisfied. Lower index 1 refers to the matrix materials, while lower index 2 refers to the inclusion materials.

The number of finite elements from the numerical results' convergence conditions was determined. To test the mesh sensitivity, Tables 1-2 were used. The parameters N_1 and N_2 indicate the number of quadrilateral finite elements along axes Ox_1 and Ox_2, respectively.

Tables 1-2 show the first fundamental frequencies (i.e., $\omega_{cr.I}^2$) for several N_1 and N_2, respectively, under the following

conditions: $R/L = 0.00625, f = 0.04, E_2/E_1 = 1, q/E_1 = 0$ and $H/L = 0.075$. Tables 1-2 reveal that the first fundamental frequencies increase with increasing values of parameters N_1 and N_2; however, it should be noted that these values only increase until they reach a certain limit. The results indicate that the mesh sensitivity used to determine the numerical solution is reliable. For the current model, the numerical results utilized 956 rectangular finite elements, with $N_1 = 80$ and $N_2 = 12$. FEM modeling was used, and the numerical results utilized 956 quadrilateral finite elements, 16 curvilinear triangular finite elements, 4041 nodes and 8032 number degrees of freedom NDOFs (Fig. 2).
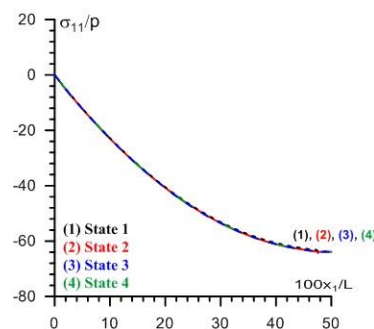
Table 1. Fundamental frequencies ($\omega_{cr.I}^2$) calculated with various values of N_1 for $N_2 = 12$.

N_1	40	50	60	70	80	85	90	100
$\omega_{cr.I}^2$	0.0333	0.0337	0.0339	0.0339	0.0340	0.0340	0.0340	0.0340

Table 2. Fundamental frequencies ($\omega_{cr.I}^2$) calculated with various values of N_2 for N_1=80.

N_2	6	8	10	12	14	16
$\omega_{cr.I}^2$	0.0337	0.0338	0.0339	0.0340	0.0340	0.0340

To verify the validation of the current results, the plate-strip with two inclusions can be considered as a whole plate-strip by taking the elastic constants $E_2/E_1 = 1$. The results for the stresses on the upper face of the plate-strip for 4 separate states were compared.

State 1: The plate-strip undergoes only its own weight (density f),
State 2: The plate-strip undergoes an uniformly distributed dynamic bending load (intensity correlates with the plate-strip's own weight) that is applied on the top of the plate-strip,

State 3: The modified case of State 2

The modified case is obtained by taking $p = \rho g h$ in State 2 (Timoshenko and Goodier (1970)) and adding the stresses $\sigma_{11} = 0, \sigma_{22} = \rho g y, \tau_{12} = 0$.

State 4: Analytical solution for a plate-strip without any defects [19].

FEM was used to calculate the solutions of the first three states.

The graphs in Figs. 3 and 4 show σ_{11}/p and σ_{22}/p on the top of the plate-strip for all four states. These graphs indicate that the four solutions converge in the appropriate cases, and the results of the present work are consistent with those of the analytical solution [19].

Fig. 3. Comparing σ_{11}/p at $x_2 = H$ obtained for all four states for the whole plate-strip.
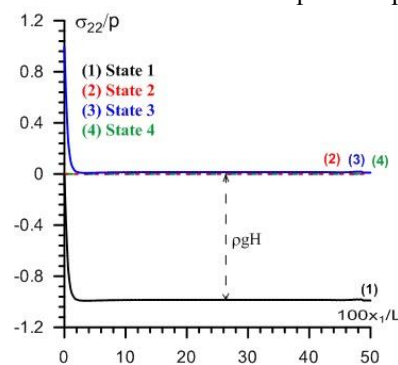

Fig. 4. Comparing σ_{22}/p at $x_2 = H$ obtained for all four states for the whole plate-strip.

Table 3 shows the first fundamental frequencies of a plate-strip that does not have inclusions for several f and q/E_1. As f decreases, the fundamental frequencies increase significantly. The first fundamental frequencies are close to the asymptotic values obtained for the plate-strip with neglected own weight. This approximation indicates that the programs and algorithms proposed by the author of the

current study are valid.

Table 3. The values of fundamental frequencies ($\omega_{cr,I}^2$) for several values of f and q/E_1 under $E_2/E_1 = 1$.

f	q/E_1					
	-0.003	-0.001	0	0.001	0.003	0.005
0.04	0.0116	0.0265	0.0340	0.0415	0.0564	0.0714
0.03	0.0128	0.0277	0.0352	0.0427	0.0576	0.0726
0.02	0.0136	0.0286	0.0361	0.0436	0.0585	0.0735
0.01	0.0142	0.0291	0.0366	0.0441	0.0590	0.0740
0	0.0144	0.0293	0.0368	0.0443	0.0592	0.0742
[6]	-	-	0.0368	0.0443	0.0592	0.0742

Table 4 indicates $|q_{cr}|/E_1$ at several f and $\bar{\omega}^2$ under $E_2/E_1 = 5$ and d/R=6. The values of $|q_{cr}|/E_1$ are calculated with the initial imperfection criterion as follows:

$$\left| u_2'^1 \big|_{\substack{x_1=L/2 \\ x_2=H}} \right| \to \infty \text{ as } q \to q_{cr}.$$

The critical values of compressive force $|q_{cr}|/E_1$ decrease with increasing values of f and $\bar{\omega}^2$.

Table 4. The values of $|q_{cr}|/E_1$ at several f and $\bar{\omega}^2$ under $E_2/E_1 = 5$ and d/R=6.

f	$\bar{\omega}^2$	$|q_{cr}|/E_1$
0	0	0.00492
	0.01	0.00360
	0.02	0.00225
0.01	0	0.00489
	0.01	0.00356
	0.02	0.00222
0.02	0	0.00482
	0.01	0.00349
	0.02	0.00215
0.04	0	0.00454
	0.01	0.00321
	0.02	0.00187

Table 5 indicate interactions between inclusions (i.e., d/R) using the values of $\sigma_{\theta\theta}/p$ for $\bar{\omega}^2 = 0.02$ where $\bar{\omega}^2$ introduces the dimensionless frequency $\bar{\omega}^2 = \omega^2 \rho L/A_{22}$ $(< \omega_{cr,I}^2)$ ($A_{22} = \lambda_k + 2\mu_k$). The values of the upper number (lower number) of the ratios indicates the values of the stresses under f=0 (f=0.04). To obtain numerical results, it is assumed that $\nu^{(1)} = \nu^{(2)} = 0.3$, R/L = 0.00625 and H/L = 0.075, unless otherwise noted. The numerical results shown in Table 5 indicate that the absolute values of the stresses decline with q/E_1, and when the effect of the plate-strip's own weight is taken into consideration, the values of the stresses are more significantly affected by the change in d/R.

Table 5. The values of stresses $\sigma_{\theta\theta}/p$ ($\sigma_{\theta\theta}/p|_{f=0}/\sigma_{\theta\theta}/p|_{f=0.04}$) are calculated for several d/R and q/E_1 values in defined angles around the circular inclusion under $E_2/E_1 = 5$ and $\bar{\omega}^2 = 0.02$.

q/E_1	θ	d/R					
		36	20	12	6	2	1
0	0	−8.2393	−8.4748	−8.5254	−8.5246	−8.4944	−8.5420
		−589.2347	−187.9667	−172.4904	−167.9380	−155.5693	−155.4949
	$\pi/4$	21.1525	27.2975	29.2177	30.1335	30.1929	29.4676
		−254.1220	−73.4935	−66.1381	−63.4337	−55.1924	−56.0394
	$\pi/2$	−30.4678	−35.3926	−36.8151	−37.4120	−37.5110	−37.1173
		−127.0534	−71.4854	−71.0687	−71.6472	−73.1866	−74.5316
	$3\pi/4$	49.2407	59.7899	62.8024	64.0405	64.0202	63.0882
		160.4307	28.4763	6.9557	−7.3569	−6.6766	−3.6923
0.005	0	−7.0307	−7.0890	−7.1008	−7.0929	−7.0847	−7.1345
		−47.8312	−48.4199	−49.0550	−48.8506	−45.8201	−46.0348
	$\pi/4$	2.5702	4.2471	4.7545	4.9969	4.9960	4.7518
		−23.0730	−21.4255	−21.1950	−20.8336	−18.6968	−19.2549
	$\pi/2$	−13.0105	−14.3296	−14.6993	−14.8530	−14.8811	−14.7684
		−14.3101	−20.4768	−22.1351	−22.7564	−23.2693	−23.6297
	$3\pi/4$	11.1749	14.0129	14.8001	15.1232	15.1108	14.8244
		4.6482	1.5025	−2.5472	−5.9610	−5.8166	−5.3257

The effect of the plate-strip's own weight, i.e., f, on the stresses (a) σ_{rr}/p, (b) $\tau_{r\theta}/p$ and (c) $\sigma_{\theta\theta}/p$ around the inclusions (in Fig. 5) and displacements (a) u_r/L and (b) u_θ/L around the inclusions (in Fig. 6) and displacements (a) u_1/L and (b) u_2/L on the plate-strip's upper face (in Fig. 7) are presented in Figs. 5-6 and 7, respectively for which $E_2/E_1 = 5$, $\bar{\omega}^2 = 0.02$ and d/R=6. In these figures, not only are the graphs presented related to the case where the value of the dimensionless pre-stretching load differ from zero, i.e., $q/E_1 = 0.005$ (solid lines), but the graphs are also related to the case where the value of the dimensionless pre-stretching load is equal to zero, i.e., $q/E_1 = 0$ (dashed lines).
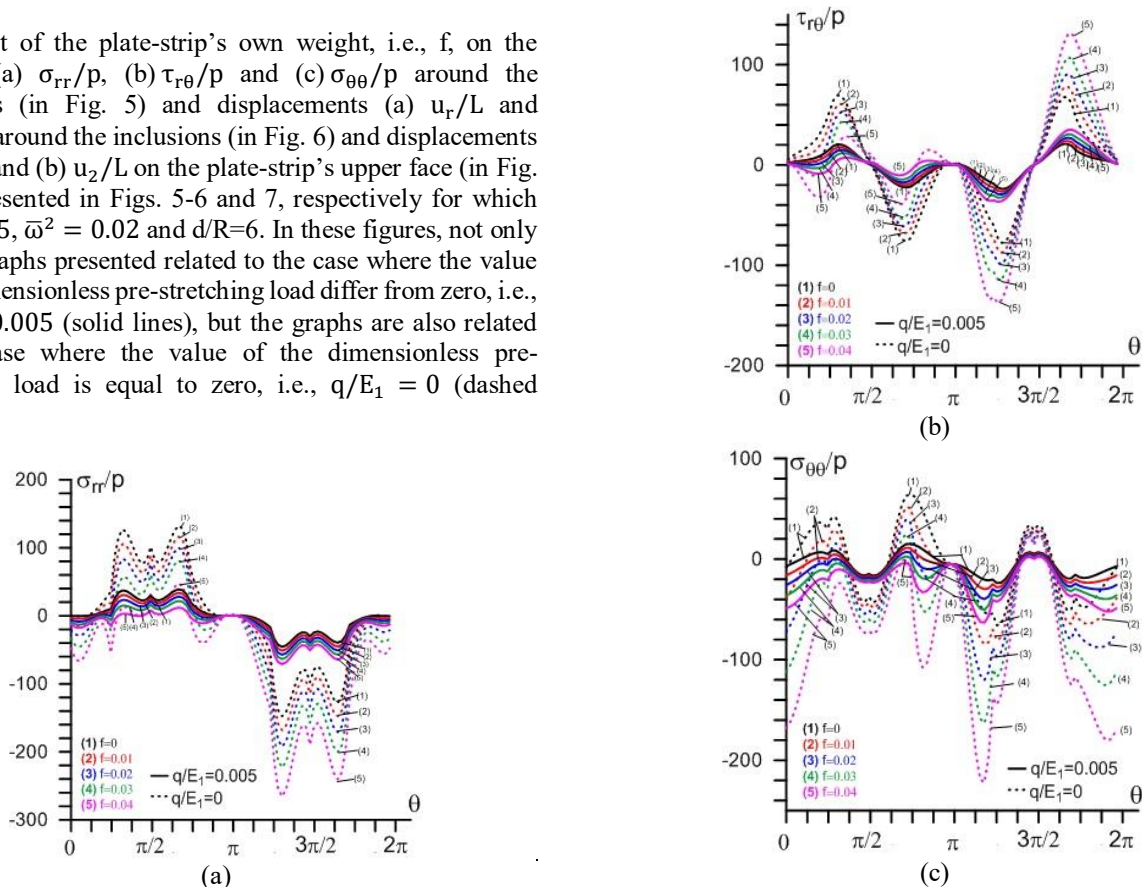

(b)

(a)

(c)

Fig. 5. Effect of f on (a) σ_{rr}/p, (b) $\tau_{r\theta}/p$ and (c) $\sigma_{\theta\theta}/p$ around the inclusions at r=R.

Figs. 5 indicate that the absolute values of stresses $\sigma_{\theta\theta}/p$ increase with density of own weight f, while the absolute values of stresses σ_{rr}/p and $\tau_{r\theta}/p$ decrease with density of own weight at $\theta\epsilon(0,\pi)$, but increase at $\theta\epsilon(\pi,2\pi)$ around the inclusions. Figs. 6 indicate that the absolute values of the displacements u_r/L and u_θ/L increase with density of own weight at $\theta\epsilon(0,\pi)$, but decrease at $\theta\epsilon(\pi,2\pi)$ around the inclusions. $\theta\epsilon(0,\pi)$ and $\theta\epsilon(\pi,2\pi)$ represent the areas closer to the inclusions upper and lower plane, respectively.

Results for all the stresses and displacements achieved for pre-stretching load i.e. $q/E_1 \neq 0$ are less than the values for $q/E_1 = 0$.

(a)

(b)
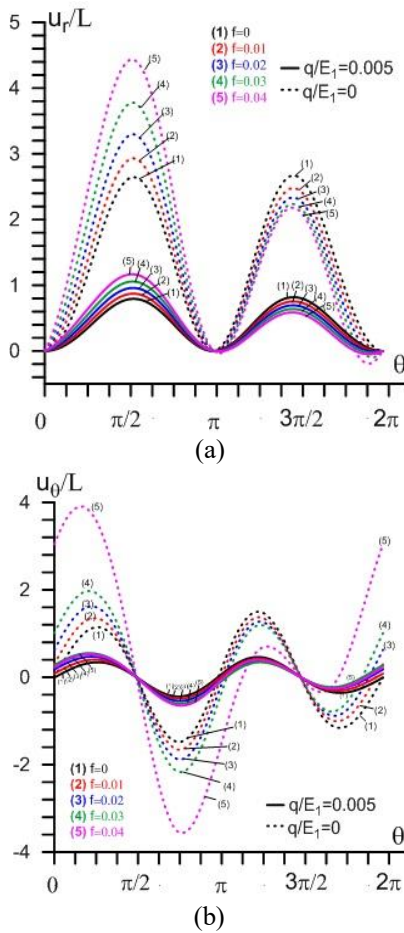
Fig. 6. Effect of f on (a) u_r/L and (b) u_θ/L around the inclusions at r=R.

Fig. 7 indicate that the displacements' absolute values are higher monotonically in cases of higher f on the plate-strip's upper face.

(a)

(b)
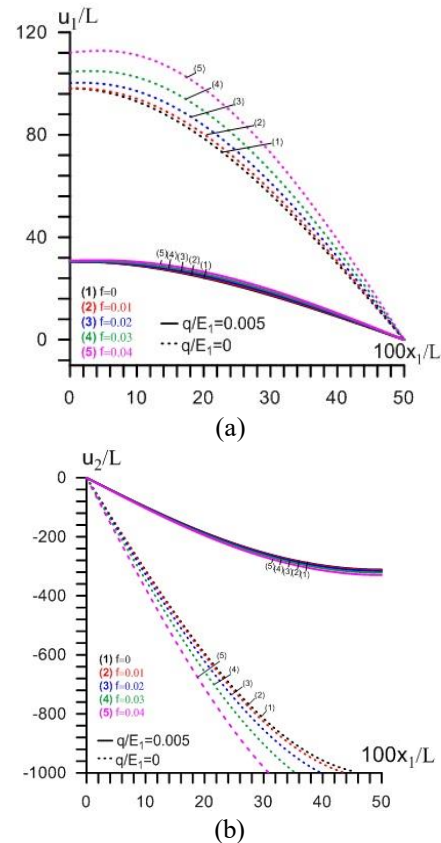
Fig. 7. Effect of f on (a) u_1/L and (b) u_2/L at $x_2 = H$ along the Ox_1 axis.

The following figures present graphs in which the plate-strip's own weight density is equal to 0.04 (solid lines), and those in which the plate-strip's own weight is neglected i.e., f=0 (dashed lines). The graphs presented in Figs. 8 and 9 examine the effect of dimensionless frequencies $\bar{\omega}^2$ on the stresses (a) σ_{rr}/p, (b) $\tau_{r\theta}/p$ and (c) $\sigma_{\theta\theta}/p$ (in Fig. 8) and displacements (a) u_r/L and (b) u_θ/L (in Fig. 9), respectively, around the inclusions at r=R, for which, $E_2/E_1 = 5$, d/R=6 and $q/E_1 = 0.005$. The graphs indicate that both the absolute values of stresses (in Fig. 8) and the displacements (in Fig. 9) around the inclusions increase with increasing $\bar{\omega}^2$. The stress and displacement values are not symmetrical with respect to π if the plate-strip's own weight is taken into account; however, they are symmetrical with respect to π if the plate-strip's own weight is neglected.
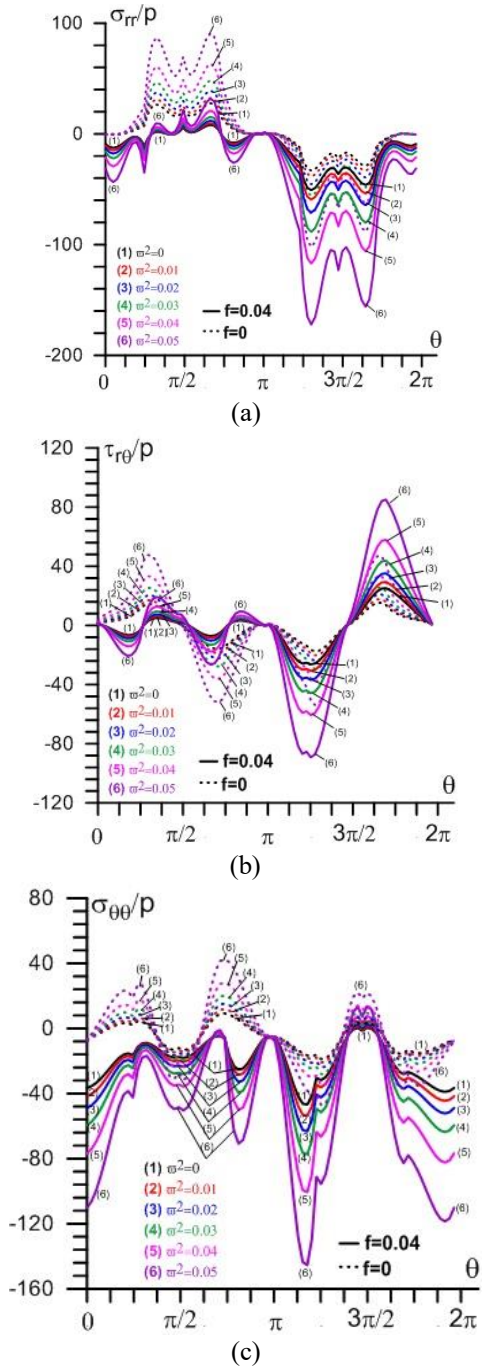
(a)

(b)

(c)

Fig. 8. Effect of $\bar{\omega}^2$ on (a) σ_{rr}/p, (b) $\tau_{r\theta}/p$ and (c) $\sigma_{\theta\theta}/p$ around inclusions at r=R.
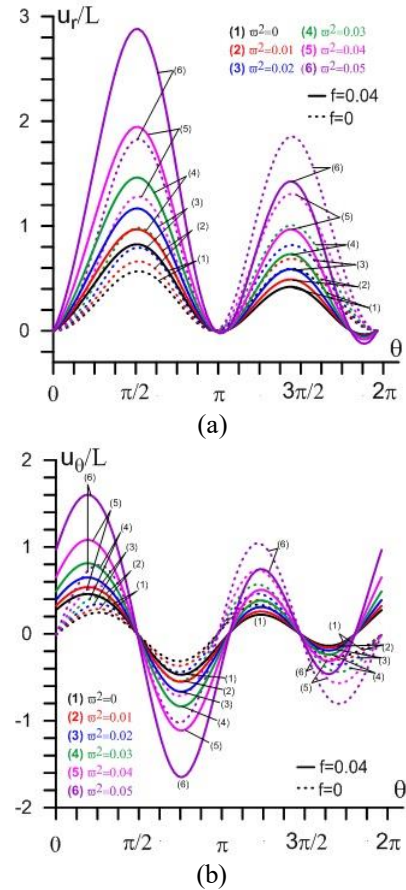

(a)

(b)

Fig. 9. Effect of $\bar{\omega}^2$ on (a) u_r/L and (b) u_θ/L around the inclusions at r=R.

The graphs presented in Fig. 10 can be used to examine the effect of dimensionless frequencies $\bar{\omega}^2$ on the values of (a) u_1/L and (b) u_2/L, respectively, on the plate-strip's upper face, for which, $E_2/E_1 = 5$, d/R=6 and $q/E_1 = 0.005$. The graphs indicate that the displacement's absolute values increase with increasing $\bar{\omega}^2$ and that the differences between the values obtained at f=0 and f=0.04 also increase with $\bar{\omega}^2$.
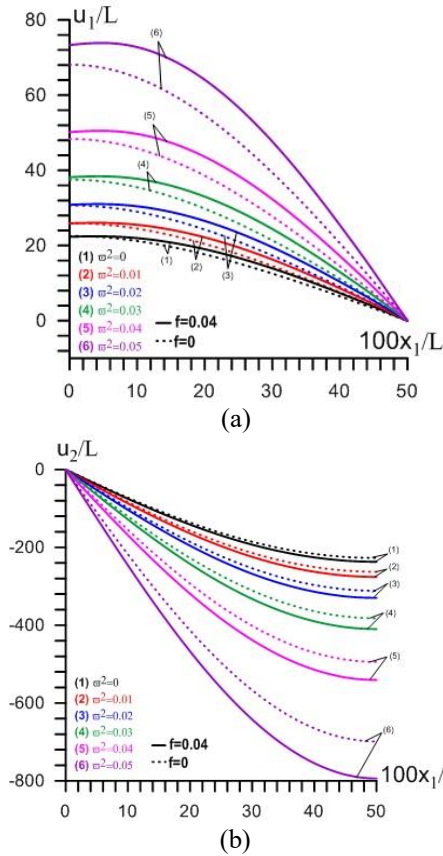
Fig. 10. Effect of $\bar{\omega}^2$ on (a) u_1/L and (b) u_2/L at $x_2 = H$ along the Ox_1 axis.

The graphs presented in Figs. 11 and 12 examine the effect of pre-stretching load q/E_1 on the stresses (a) σ_{rr}/p, (b) $\tau_{r\theta}/p$ and (c) $\sigma_{\theta\theta}/p$ (in Fig. 11) and displacements (a) u_r/L and (b) u_θ/L (in Fig. 12), respectively, for which $E_2/E_1 = 5$, $\bar{\omega}^2 = 0.02$ and d/R=6. Results indicate that the absolute values of displacements and stresses decrease significantly with pre-stretching load, i.e., q/E_1 and this effect is greater when considering the plate-strip's own weight.
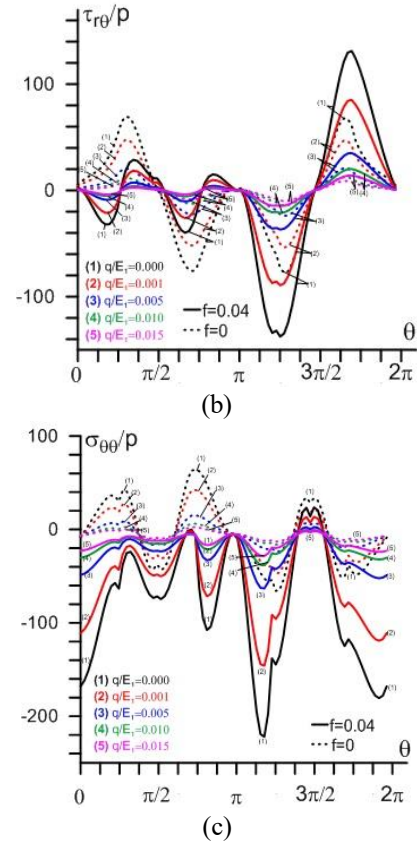
Fig. 11. Effect of q/E_1 on (a) σ_{rr}/p, (b) $\tau_{r\theta}/p$ and (c) $\sigma_{\theta\theta}/p$ around inclusions at r=R.
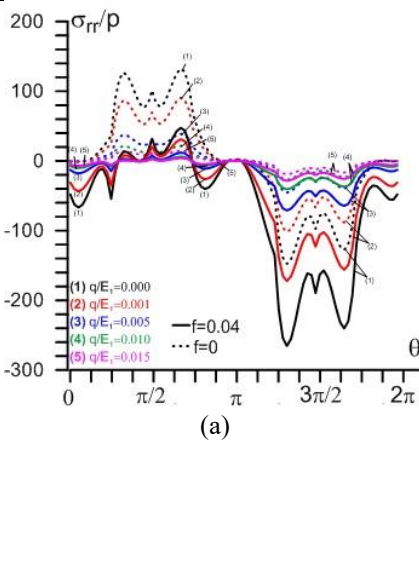

Fig. 12. Effect of q/E_1 on (a) u_r/L and (b) u_θ/L around inclusions at r=R.

The graphs presented in Fig. 13 examine the effect of q/E_1 on the displacements (a) u_1/L and (b) u_2/L, respectively, along the Ox_1 axes on the plate-strip's upper face, under the conditions $E_2/E_1 = 5$, $\bar{\omega}^2 = 0.02$ and d/R=6, for both cases of f. The graphs indicate that the absolute values of displacements u_1/L and u_2/L, decrease with q/E_1, and the differences between the values obtained at f=0 and f=0.04 decrease with q/E_1.
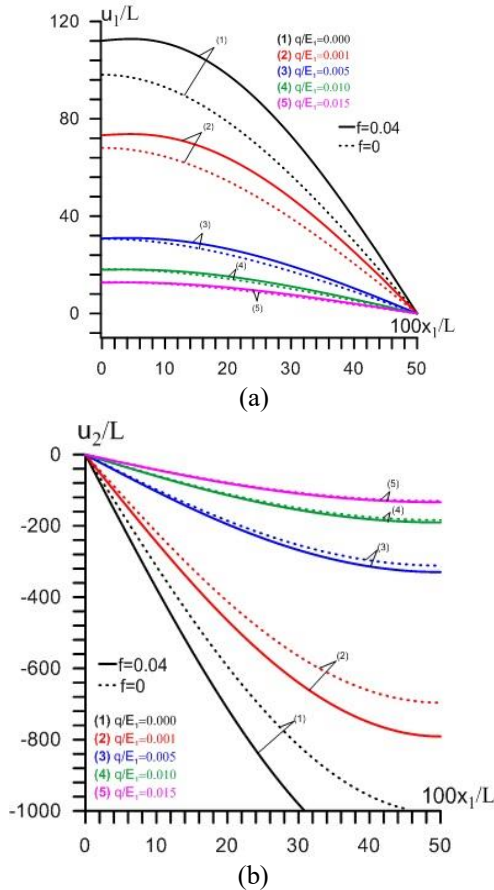

Fig. 13. Effect of q/E_1 on (a) u_1/L and (b) u_2/L at $x_2 = $ H.

The graphs presented in Fig. 14 indicate the effect of E_2/E_1 on the stresses (a) σ_{rr}/p, (b) $\tau_{r\theta}/p$ and (c) $\sigma_{\theta\theta}/p$ for which $q/E_1 = 0.005$, $\bar{\omega}^2 = 0.02$ and d/R=6. Results indicate that change of E_2/E_1 affects the absolute values of the stresses around the inclusions significantly. The absolute values of all the stresses around the inclusion increase with E_2/E_1. Although the absolute values of stresses obtained for f = 0 are greater than those obtained for f = 0.04 at $\theta \epsilon(0, \pi)$, the values obtained for f= 0.04 are greater than those obtained for f = 0 at $\theta \epsilon(\pi, 2\pi)$.
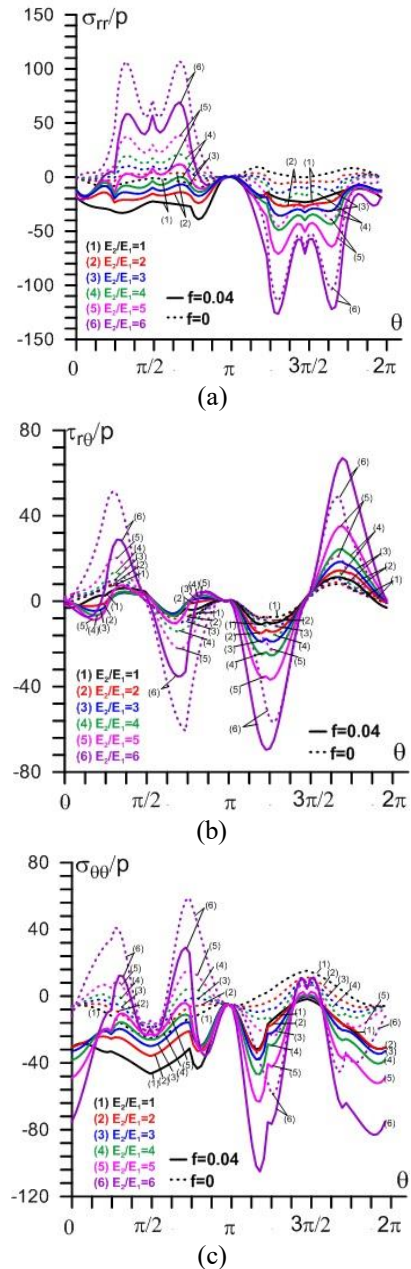

Fig. 14. Effect of E_2/E_1 on (a) σ_{rr}/p, (b) $\tau_{r\theta}/p$ and (c) $\sigma_{\theta\theta}/p$ around inclusions at r=R.

The graphs presented in Figs. 15 and 16 examine the effect of the varied upward replacement of the inclusions positions (i.e., effect of parameter H_T/R) on the stresses (a) σ_{rr}/p, (b) $\tau_{r\theta}/p$ and (c) $\sigma_{\theta\theta}/p$ (in Fig. 15) and displacements (a) u_r/L and (b) u_θ/L (in Fig. 16) respectively, for which $E_2/E_1 = 5$, $\bar{\omega}^2 = 0.02$, d/R=6 and $q/E_1 = 0.005$. Results indicate that the absolute values of displacements and stresses increase significantly with lower H_T/R for f=0 and f=0.04.
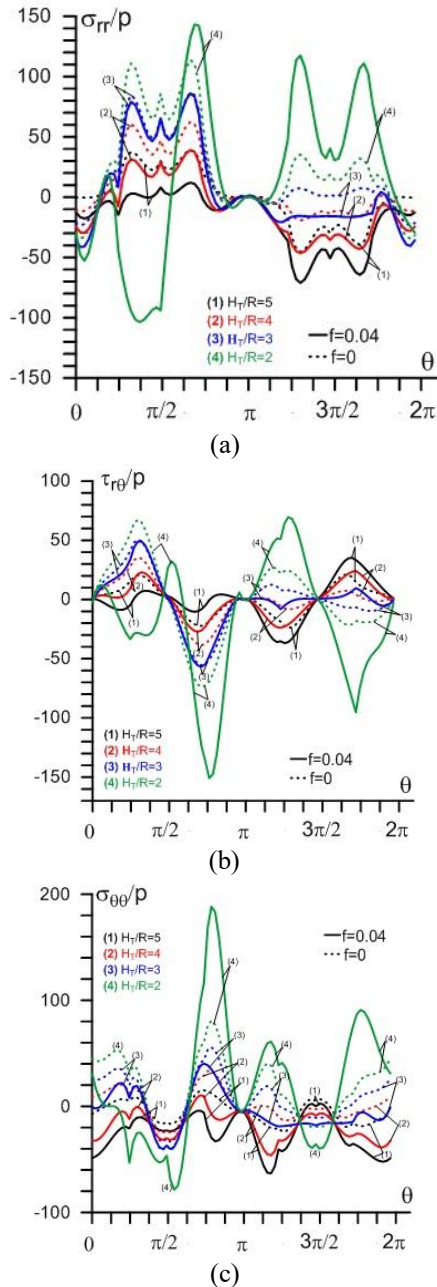
Fig. 15. Effect of H_T/R on (a) σ_{rr}/p, (b) $\tau_{r\theta}/p$ and (c) $\sigma_{\theta\theta}/p$ around inclusions at r=R.
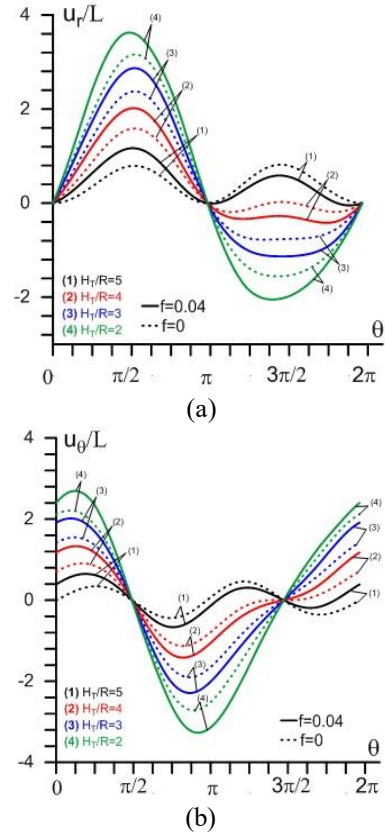

Fig. 16. Effect of H_T/R on (a) u_r/L and (b) u_θ/L around the inclusions at r=R.

5. CONCLUSIONS

This study aimed to identify the effects of own weight of a plate-strip containing twin circular inclusions to dynamic analyses under bending conditions. Centers of inclusions are on a line parallel to the free surface and made from the same materials. The effects of body forces (own weight) and surface forces (pre-stretching load) have been considered together as the initial stresses can be determined via the classical linear theory of elasticity. The effects of these initial stresses on dynamic analyses around the inclusions within a plate-strip under additional time harmonic bending load are studied via the TDLTE taking into account the state of the plane strain. Within this study the best way to determine the solution was analyzed, and an algorithm was designed to determine the numerical results. According to the study the following conclusions can be reached:

- First fundamental frequencies decrease with the plate-strip's own weight and increase with initial stretching force.
- When the effect of the plate-strip's own weight is taken into consideration, the values of the stresses are more significantly affected by the change in d/R (distance between two inclusions).
- The values of $|q_{cr}|/E_1$ decrease with f and $\overline{\omega}^2$ ($< \omega_{cr.I}^2$).
- The values of $|\sigma_{\theta\theta}/p|, |\sigma_{rr}/p|, |\tau_{r\theta}/p|, |u_r/L|$ and u_θ/L around the inclusions increase with dimensionless frequencies $\overline{\omega}^2$.
- The values of $|u_1/L|$ and $|u_2/L|$ on the plate-strip's upper face increase with dimensionless frequencies $\overline{\omega}^2$ and the differences between the values obtained at f=0 and f=0.04 increase with $\overline{\omega}^2$.
- The values of $|\sigma_{\theta\theta}/p|$ around the inclusions increase with increasing density of own weight f.
- The values of $|\sigma_{rr}/p|, |\tau_{r\theta}/p|$ around the inclusions decrease with density of own weight at $\theta\epsilon(0,\pi)$, but increase at $\theta\epsilon(\pi,2\pi)$.
- The values of $|u_r/L|$ and $|u_\theta/L|$ around the inclusions increase when taking into account the density of own weight at $\theta\epsilon(0,\pi)$, but decrease at $\theta\epsilon(\pi,2\pi)$.
- The values of $|u_1/L|$ and $|u_2/L|$ on the plate-strip's upper face increase with density of own weight and this effect is greater for the case $q/E_1 = 0$.
- The stresses' and displacements' absolute values around the inclusions are significantly decrease with pre-stretching force q/E_1, and this effect is greater when considering plate-strip's own weight.
- The absolute values of stresses around the inclusions increase with E_2/E_1.
- The stresses' absolute values obtained for f=0 are greater than those obtained for f =0.04 at $\theta\epsilon(0,\pi)$, but the values obtained for f = 0.04 are greater than those obtained for f=0 at $\theta\epsilon(\pi,2\pi)$.
- The stresses' and displacements' absolute values are significantly greater in cases where the upward replacement of the position of the inclusions, i.e., H_T/R, decrease for the cases f=0 and f=0.04.

ACKNOWLEDGEMENTS

REFERENCES

[1] T. Mura, "Inclusion problems", Appl. Mech. Rev., vol. 41, no 1, pp. 15-20, 1988.

[2] T. Mura, H.M. Shodja and Y. Hirose, "Inclusion problems", Appl. Mech. Rev., vol. 49, no 10S, pp. 118-127, 1996.

[3] K. Zhou, H.J. Hoh, X. Wang, L.M. Keer, J.H.L. Pang, B. Song and Q.J. Wang, "A review of recent works on inclusions", Mech. Mater., vol. 60, pp. 144-158, 2013.

[4] W. Hufenbach and B. Zhou, "Solutions for an anisotropic finite plate with an elastic inclusion and a loaded boundary", Compos. Struct., vol. 52, no 2, pp. 161-166, 2001.

[5] J.H. Huang, "Vibration response of laminated plates containing spheroidal inclusions", Compos. Struct., vol. 50, no 3, pp. 269-277, 2000.

[6] U. Babuscu Yesil, "Forced vibration analysis of pre-stretched plates with twin circular inclusions", J. Eng. Mech., vol. 141, no 1, pp. 04014099-1-04014099-16, 2015.

[7] S.D. Akbarov, Dynamics of Pre-Strained Bi-Material Elastic Systems Linearized Three-Dimensional Approach, Springer-Heidelberg, New York, 2015.

[8] H. Takabatake, "Effects of dead loads in dynamic plates", J. Struct. Eng.-ASCE, vol. 118, no 1, pp. 34-51, 1992.

[9] H. Takabatake, "Effects of dead loads on dynamic analyses of beams subject to moving loads", Earthq. Struct., vol. 5, no 5, pp. 589-605, 2013.

[10] H. Takabatake, "Effect of dead loads on natural frequencies on beams", J. Struct. Eng.-ASCE, vol. 117, no 4, pp. 1039-1052, 1991.

[11] H. Takabatake, "Effects of dead loads on dynamic analyses of beams", Earthq. Struct., vol. 1, no 4, pp. 411-425, 2010.

[12] U. Babuscu Yesil, "The effect of own weight on the static analysis of a pre-stretched plate-strip with a circular hole in bending", Mech. Compos. Mater., vol. 53, no 2, pp. 243-252, 2017.

[13] S.J. Zhou and X. Zhu, "Analysis of effect of dead loads on natural frequencies of beams using finite-element techniques", J. Struct. Eng. -ASCE, vol. 122, no 5, pp. 512-516, 1996.

[14] S.J. Zhou, "Load-induced stiffness matrix of plates", Can. J. Civ. Eng., vol. 29, no 1, 181-184, 2002.

[15] S.D. Akbarov, Stability Loss and Buckling Delamination: Three-Dimensional Linearized Approach for Elastic and Viscoelastic Composites, Springer-Heidelberg, New York, 2013.

[16] A.N. Guz, Fundamentals of the Three-Dimensional Theory of Stability of Deformable Bodies, Springer-Verlag, Berlin, 1999.

[17] A.N. Guz, Elastic Waves in Bodies with Initial (Residual) Stresses [in Russian], Kiev, 2004.

[18] O.C. Zienkiewicz and R.L. Taylor, The Finite Element Methods: Basic Formulation and Linear Problems (Vol. 1, 4th Edition). Mc Graw-Hill Book Company, Oxford, 1989.

[19] S.P. Timoshenko and J.N. Goodier, Theory of Elasticity, Third Edition, McGraw-Hill International Editions, London, 1970.